

# Scattering of hydrogen ions and atoms of energy $\sim 1$ MeV in gases without charge changing

V. I. Radchenko

*S. M. Kirov Ural Polytechnic Institute*

(Submitted 15 April 1992; resubmitted 15 August 1992)

Zh. Eksp. Teor. Fiz. **103**, 40–49 (January 1993)

Scattering of fast hydrogen particles  $H^-$ ,  $H^0$ , and  $H^+$  in gases without charge changing is studied. The experimental setup and procedure are described, and total scattering cross sections for these particles of energy  $E = 0.71, 1.15$  and  $1.67$  MeV in He, Ar, Kr, Xe,  $H_2$ ,  $O_2$ , and  $CO_2$  are listed. For a helium target, in the bombarding-particle energy range  $E = 0.1$ – $15$  MeV, the differential and total cross sections, as well as characteristic angles of scattering without charge changing for hydrogen particles and for particles created when  $H^-$  ions lose electrons in collisions, are calculated. Experimental and theoretical data are analyzed and compared with each other.

## INTRODUCTION

As is well-known,<sup>1</sup> studies of processes of elastic and inelastic scattering, in which the charge of incident particles is conserved, play a fundamental role in the physics of ion-atom interactions. This stems from the fact that these processes are important both for construction and verification of theoretical models and for solution of practical problems.

Among the problems connected with the development of accelerators, storage rings, installations for controlled thermonuclear fusion using ion beams, to transport of particle beams over significant distances, etc., one of the focal points is the dynamics of the beam phase volume due to ion-atom collisions. The growth of the beam volume in phase space is often equivalent to particle loss and lowers installation efficiency.

In the context of the formulated problem, particle scattering at small angles ( $\lesssim 10^{-3}$  rad), involving energies of order 0.1 to  $\sim 10$  MeV per nucleon without charge changing, are of interest. The theoretical and experimental data available in the literature concerning differential cross sections and other quantities needed for description of these processes, are inadequate. As a rule, these data relate to processes of excitation of an incident particle, as well as excitation and/or ionization of a target. However, the main role is played mostly by the differential and total effective cross sections of scattering without charge changing, in an integral form, over separate channels of reaction, i.e. by the cross sections, which characterize the whole set of phenomena in which the incident particle charge is conserved, while the state of particle electron shell, as well as the particle-target state (both charge and structural), can vary in an arbitrary manner. We denote the scattering of particles of charge  $i$  without charge changing by  $(ii)$ .

Experimental study of total cross sections  $\sigma_{ii}$  in their form integral, over  $(ii)$ -processes, (it is these cross sections that are basically discussed in this paper) is based upon the measurement of spatial-angular distribution (SAD) of particles. Let us illustrate this by an example. Let the characteristic angles of  $(ii)$ -scattering be much larger than the angular spread of the initial ion beam. Then, in the detection plane, the SAD of the ions which have undergone collisions of  $(ii)$ -type at the target will be much wider than that of

particles, which have not interacted with the target (the latter distribution corresponds to the apparatus function (AF) of the installation). The resulting SAD has the form of a narrow peak formed by particles, which have passed through the target without “noticing” it, located on a wide plane “pedestal” formed by particles scattered in the target. Thus, we can separate the fraction of particles with initial angular divergence from that of particles scattered in  $(ii)$ -collisions. As a result, it is not difficult to show that if the fraction  $\Phi_i^V(t)$  of particles, changing and then restoring their initial charge, as they pass through the target, is negligible, we have

$$\sigma_{ii} = \frac{1}{t} \ln \frac{j_i^{(0)}(0)}{j_i^{(0)}(t)}, \quad (1)$$

where  $j_i^{(0)}(0)$  and  $j_i^{(0)}(t)$  are the heights of the distribution peaks for particles with initial divergence above the pedestal for the AF ( $t = 0$ ) and after passing through a target of thickness  $t$ . The peak heights must be normalized to the same number of particles detected in each measurement.

The aim of the present study is to determine experimentally the cross section  $\sigma_{ii}$  for scattering of hydrogen particles  $H^+$ ,  $H^-$ , and  $H^0$  of energy  $E = 0.71, 1.15,$  and  $1.67$  MeV, without charge changing, in the following He, Ar, Kr, Xe,  $H_2$ ,  $O_2$ , and  $CO_2$ . As far as we know, there are no reports of such measurements. This is partially explained by that such measurements require development of installations having small (in absolute value) beam divergence and small angular resolution.

## EXPERIMENTAL SETUP AND MEASUREMENT RESULTS

The diagram of the experimental setup is shown in Fig. 1. Protons and ions were accelerated in a classical R-7 (U-120) cyclotron. The intensity of the extracted beam was  $\sim 0.1$ – $1 \mu A$ . A turning SP-45 magnet directed the ion beam into a test channel with a vacuum of  $\lesssim 10^{-4}$  Pa maintained over its entire length. The beam was collimated by two slit diaphragm S11 and S12 of height  $20 \mu m$  each. The particles were detected by a DKPs-350 semiconductor detector with an entrance-slit collimator of height  $10 \mu m$ . Thus, the beam divergence and angular resolution of the installation were

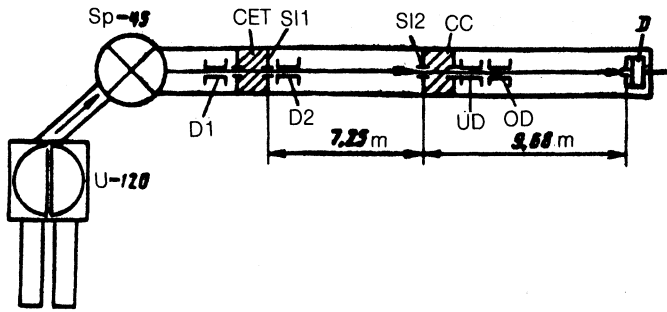


FIG. 1. Diagram of the experimental setup.

$\sim 3 \cdot 10^{-6}$  and  $5 \cdot 10^{-6}$  rad (for the SAD width at half the height) respectively.

Angular distributions were measured for beams of ribbon geometry (for ribbon width of order  $\approx 8$  mm). Certainly, if we use beams with circular or square cross-section of sufficiently small size, we get more information, i.e., we can find directly the differential cross section of this or that studied process. But in our case we cannot use them due to the drastic decrease in collimated beam intensity and to more stringent requirements on the means of beam control.

A beam of ions accelerated in a cyclotron and having a required charge was produced using a charge-exchange gas target S11 CET installed in the front of the first slit SI1 and by electric D1 and D2 deflectors dividing (D2) the beam into charge fractions and directing the required one to the second collimating slit SI2.

The interaction between the particle beam and gas target occurred in a collision chamber CC of length 390 mm, which had the slit SI2 as its entrance window and a slit of height  $300 \mu\text{m}$  to restrict the gas flow as its exit window. The gas entered through an SNA-1 piezoelectric leak valve up to a pressure 0.1–3 Pa, measured with a calibrated PMI-10-2 manometric converter with a VIT-3 instrument. The effective target thickness thus found was in error by 5 to 7%.

The measurement of the SAD of beam components with a definite ion charge was carried out by electric UD and OD deflectors. The procedure and electronic equipment for measurement of ion beam profile are described in Ref. 2. To measure the SAD of hydrogen atoms we used a detector *D* with a fixed slit, which could be mechanically displaced by a given distance. The displacement range was 0...9 mm with a  $1.6 \mu\text{m}$  pitch. The necessary monitoring of the total particle flux was carried out with the help of a detector with a collimating slit made of a thin foil. The ions, passing through the foil, lost some energy, which made it possible, by using particle energy spectrometry, to separate those ions which hit the target. The detector acceptance was much larger than the beam emittance.

The typical SAD curves measured for the AF ( $t = 0$ ) of the setup and for particles which have passed through the gas target are shown in Fig. 2. The scattering cross sections  $\sigma_{ii}$  for fast hydrogen particles calculated with the help of Eq. (1) are listed in Table I. The values of experimental error  $\sigma$  corresponding to one standard deviation are also listed there.

With allowance for experimental errors, the cross sections obtained obey the following laws:

1. For fixed energy of the incident particles we have

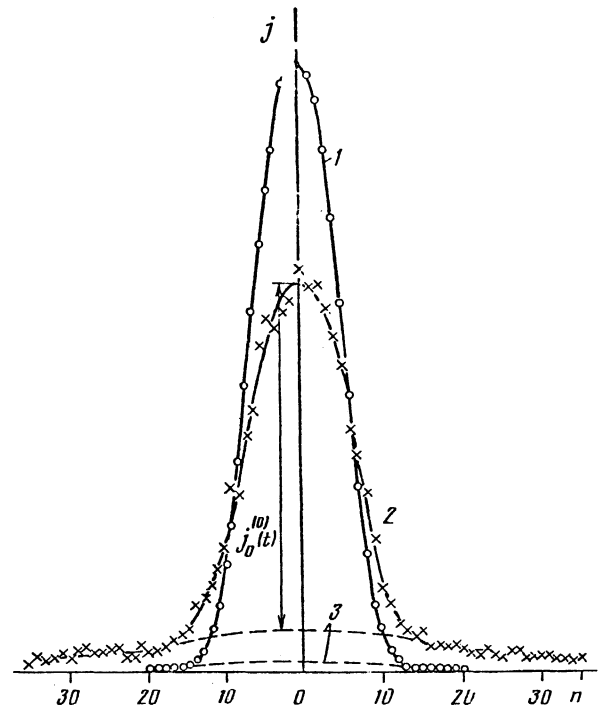


FIG. 2. Spatial-angular distributions  $j(n)$  of  $\text{H}^-$  ions with energy  $E = 0.71$  MeV ( $n$  is the channel number<sup>2</sup>). Curve 1: the setup apparatus function,  $t = 0$ ; curve 2: the SAD for a helium target,  $t = 1.81 \cdot 10^{16} \text{ cm}^{-2}$ ; curve 3: "pedestal". The number of particles detected in distributions 1 and 2 is the same.

$\sigma_{11} > \sigma_{\bar{1}\bar{1}} > \sigma_{00}$  for all gas targets studied.

2. For any  $i$  the cross sections  $\sigma_{ii}$  for every value of  $E$  increase with the atomic number of monatomic gases with the atomic numbers of particles entering into the composition of molecular targets.

3. For the same target, the cross-sections  $\sigma_{ii}$  decrease in a monotonic manner with collision energy for all  $i$ .

Note also that the cross sections  $\sigma_{ii}$  obtained are close to, though somewhat smaller than, the corresponding electron-loss cross sections<sup>3</sup>:  $\sigma_{\bar{1}\bar{1}} \lesssim \sigma_{\bar{1}0}$  and  $\sigma_{00} \lesssim \sigma_{01}$ . This raises interest in the angular characteristics of ( $\bar{1}\bar{1}$ )-processes, since for comparable particle-scattering angles with and without charge change collisions of ( $\bar{1}\bar{1}$ )- and (00)-type substantially affect the formation of a hydrogen atom beam upon neutralization of hydrogen ions  $\text{H}^-$ .

## CROSS-SECTION CALCULATION AND DISCUSSION

To compare the characteristic scattering angles for fast hydrogen particles in ( $\bar{1}0$ ), ( $\bar{1}\bar{1}$ ), and (00) processes and to get an idea of the value of relevant total cross sections (the same for (11)-collisions), we calculate differential cross sections of these processes for a helium target in the Born approximation, making use of the approach suggested in Ref. 4. For two colliding systems *A* and *B*

$$A(\alpha_i) + B(\beta_i) \rightarrow A(\alpha_f) + B(\beta_f), \quad (2)$$

where  $\alpha_i, \beta_i$  and  $\alpha_f, \beta_f$  are initial and final states, the differential cross sections of scattering at an angle  $\theta$  in the lab, summed over all possible final states  $\beta_f$  of the target, is written in the form

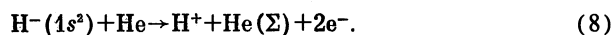
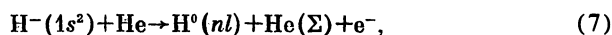
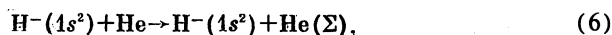
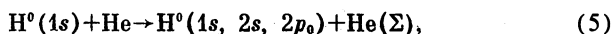
TABLE I. Experimental scattering cross sections for fast hydrogen particles in gases without charge changing ( $\cdot 10^{-18}$  cm<sup>2</sup>). The index (*T*) denotes the line containing theoretical cross sections  $\sigma_{ii}$  calculated in the present study. 1: MeV; 2: gas.

E, MeV	0,71			1,15			1,67		
	$\sigma_{11}$	$\sigma_{\bar{1}\bar{1}}$	$\sigma_{\infty}$	$\sigma_{11}$	$\sigma_{\bar{1}\bar{1}}$	$\sigma_{\infty}$	$\sigma_{11}$	$\sigma_{\bar{1}\bar{1}}$	$\sigma_{\infty}$
He	39	19	9,3	34	17	8,7	27	7,5	7,0
He <sup>(n)</sup>	50,6	17,4	16,4	34,3	12,5	10,2	25,2	9,72	7,04
Ar	390	160	150	280	230	160	320	110	77
Kr	540	230	180	360	230	140	410	140	130
Xe	500	350	210	450	330	150	590	220	140
H <sub>2</sub>	120	43	21	76	40	19	47	24	7,5
O <sub>2</sub>	300	140	180	200	130	77	270	96	70
CO <sub>2</sub>	410	230	170	360	210	110	290	140	83
$\delta$ , %	25	25	25	20	25	20	20	25	25

$$\frac{d\sigma_{\alpha_f}(\theta)}{d\Omega} = \sum_{\beta_f} \frac{d\sigma_{\alpha_f\beta_f}}{d\Omega} = \frac{4a_0^2}{(\bar{q}a_0)^4} \left( \frac{M_A}{m} \right)^2 |F_{\alpha_f\alpha_i}^A(\bar{q})|^2 \times \{Z_e^B S_{inc}^B(\bar{q}) + |F_{\beta_f\beta_i}^B(\bar{q})|^2\}, \quad (3)$$

where  $a_0$  is the radius of the first Bohr orbit,  $m$  and  $M_A$  are the masses of the electron and of the system  $A$ , respectively,  $F_{\alpha_f\alpha_i}^A$  is the atomic form factor of the system  $A$ ;  $Z_e^B S_{inc}^B$  is the function of incoherent scattering of the system  $B$ , and  $\bar{q}$  is a mean value of the wave vector, which can be found by a procedure suggested in Ref. 4.

We consider the following processes



The symbol “ $\Sigma$ ” means here that all possible final states of the target, belonging both to the discrete and continuous spectra, are taken into account.

As in Ref. 4, we describe the ground state of He atoms by the Hartree–Fock wave function, and that of  $H^-$  ions by the Chandrasekar wave function

$$\Psi_{H^-} = N [\exp\{-(\alpha r_1 + \beta r_2)/a_0\} + \exp\{-(\beta r_1 + \alpha r_2)/a_0\}], \quad (9)$$

where  $\alpha = 1.04$ ,  $\beta = 0.2808$ , and  $N = 0.03115/a_0^3$  is the normalization factor. The use of the Chandrasekar wave function yields analytic expressions for the form factor and the incoherent-scattering function for  $H^-$  ions.

We list the relations for the form factors of incident particles taking part in reactions (5) and (6):

$$F_{1s^2}^{H^-}(\bar{q}) = 1 - \frac{16}{(4 + \bar{q}^2 a_0^2)^2}, \quad (10)$$

$$F_{2s^2}^{H^-}(\bar{q}) = -\frac{2^9 \bar{q}^2 a_0^2}{2^{1/2} (9 + 4\bar{q}^2 a_0^2)^3}, \quad (11)$$

$$F_{2p_0^2}^{H^-}(\bar{q}) = \frac{3 \cdot 2^8 \bar{q} a_0}{2^{1/2} (9 + 4\bar{q}^2 a_0^2)^3}, \quad (12)$$

$$F_{1s^2}^{H^-}(\bar{q}) = 1 - 2 \langle \Psi_{H^-} | e^{i\mathbf{q}\mathbf{r}} | \Psi_{H^-} \rangle, \quad (13)$$

where

$$\langle \Psi_{H^-} | e^{i\mathbf{q}\mathbf{r}} | \Psi_{H^-} \rangle = 16\pi^2 a_0^6 N^2 \left\{ \frac{\alpha}{\beta^3 (4\alpha^2 + q^2 a_0^2)^2} + \frac{\beta}{\alpha^3 (4\beta^2 + q^2 a_0^2)^2} + \frac{8}{(\alpha + \beta)^2 [(\alpha + \beta)^2 + q^2 a_0^2]^2} \right\}. \quad (14)$$

Summing (3) over  $\alpha_f \neq \alpha_i$ , we find the differential cross section for the superposition ( $\bar{1}0$ ) + ( $\bar{1}\bar{1}$ ) of processes (7) and (8), since the excited states of  $H^-$  ions are self-detaching.<sup>5</sup> Formula (3) is replaced by an expression in which, instead of the form-factor square modulus, we have the function of incoherent scattering of  $H^-$  ions:

$$S_{inc}^{H^-}(\bar{q}) = 1 + \langle \Psi_{H^-} | \exp\{i\mathbf{q}(\mathbf{r}_1 - \mathbf{r}_2)\} | \Psi_{H^-} \rangle - 2(\langle \Psi_{H^-} | \exp\{i\mathbf{q}\mathbf{r}\} | \Psi_{H^-} \rangle)^2, \quad (15)$$

where

$$\langle \Psi_{H^-} | \exp\{i\mathbf{q}(\mathbf{r}_1 - \mathbf{r}_2)\} | \Psi_{H^-} \rangle = 128\pi^2 a_0^6 N^2 \left\{ \frac{4\alpha\beta}{(4\alpha^2 + q^2 a_0^2)^2 (4\beta^2 + q^2 a_0^2)^2} + \frac{(\alpha + \beta)^2}{[(\alpha + \beta)^2 + q^2 a_0^2]^4} \right\}. \quad (16)$$

Note<sup>3,4</sup> that for  $E \geq 200$  keV the cross section  $\sigma_{\bar{1}\bar{1}}$  amounts to about 4% of  $\sigma_{\bar{1}0}$ , therefore the cross sections  $d\sigma_{(\bar{1}0) + (\bar{1}\bar{1})}/d\Omega$  and  $\sigma_{(\bar{1}0) + (\bar{1}\bar{1})}$  found in the framework of this approach with the help of Eqs. (15) and (16) allow us to get an exact idea of the angular characteristics and efficiency of neutralization of  $H^-$  ions.

The results found by means of Eqs. (10)–(16) are shown in Fig. 3 and listed in Tables II and III. The total cross sections have been found by a straightforward integration of the differential cross sections.

For processes (5) with formation of hydrogen atoms in 1s and 2s-states, the differential cross sections have a crater-like form. The differential cross sections of other processes, with the exception of the ( $\bar{1}\bar{1}$ ) process, have a bell-shaped form. In the case of ( $\bar{1}\bar{1}$ ) collisions the differential cross section, as seen from Fig. 3, has two maxima at  $\theta \geq 0$ . In the interval between them we have  $d\sigma_{\bar{1}\bar{1}}(\theta_0)/d\Omega = 0$  for a certain angle  $\theta_0$ . If the wave function (9) is used, the differential cross section of ( $\bar{1}\bar{1}$ )-process vanishes for angles  $\theta_0$  some-

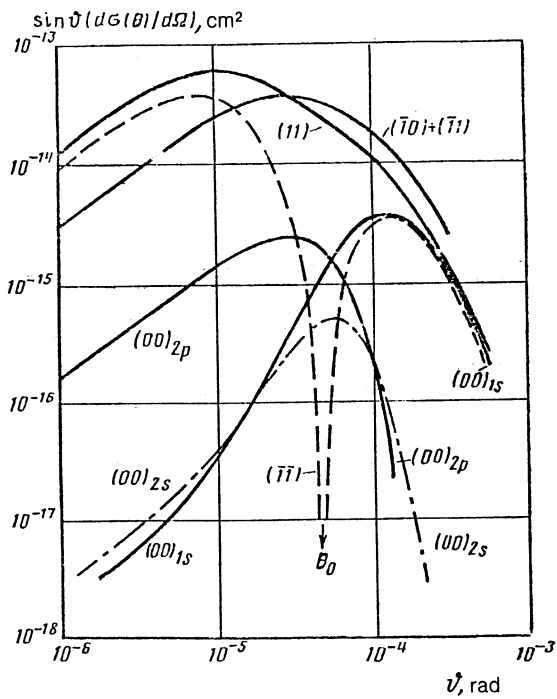


FIG. 3. Differential scattering cross sections of hydrogen particles of energy  $E = 1.67$  MeV.

TABLE II. Characteristic scattering angles for hydrogen particles in helium ( $\times 10^{-6}$  rad). 1: MeV

$E, \text{ MeV}$	$\theta_{\frac{1}{2}}^{(\bar{1}0)+(\bar{1}1)}$	$\theta_{\frac{1}{2}}^{(00)}$	$\theta_{\frac{1}{2}}^{(\bar{1}\bar{1})}$	$\theta_{\frac{1}{2}}^{(11)}$
0,1	283	490	41,9	172
0,15	177	400	47,0	115
0,2	131	345	41,6	85,9
0,3	89,9	285	32,5	57,4
0,4	70,7	245	26,6	43,0
0,6	52,2	200	19,6	28,7
0,71	46,7	185	17,2	24,2
0,8	42,9	176	15,7	21,5
1	37,1	156	13,1	17,2
1,15	34,0	147	11,7	14,9
1,67	27,2	122	8,51	10,3
2	24,6	111	7,31	8,66
3	19,6	91,0	5,10	5,75
5	14,9	71,0	3,20	3,50
6,9	12,6	60,0	2,39	2,54
10,4	10,2	49,3	1,58	1,65
14,9	8,47	41,0	1,13	1,17

TABLE III. Total scattering cross sections for hydrogen particles in He with electron detachment and without charge changing ( $\times 10^{-18}$  cm<sup>2</sup>).

$E, \text{ MeV}$	$\sigma_{(\bar{1}0)+(\bar{1}1)}$	$\sigma_{00}$	$\sigma_{00}(1s)$	$\sigma_{00}(2s)$	$\sigma_{00}(2p)$	$\sigma_{\bar{1}\bar{1}}$	$\sigma_{11}$
0,1	304	105	97,9	2,48	4,05	91,8	22,2
0,15	250	71,9	65,7	2,04	4,23	61,7	168
0,2	202	54,8	49,1	1,68	4,00	47,0	136
0,3	147	37,4	32,9	1,21	3,39	33,1	99,7
0,4	115	28,4	24,6	0,935	2,87	26,2	79,8
0,6	80,5	19,3	16,5	0,639	2,17	19,5	58,0
0,71	68,9	16,4	14,0	0,543	1,90	17,4	50,6
0,8	61,8	14,6	12,4	0,484	1,73	16,0	46,0
1	50,5	11,8	9,89	0,389	1,44	13,8	38,4
1,15	44,0	10,2	8,57	0,339	1,28	12,5	34,3
1,67	30,7	7,04	5,89	0,235	0,916	9,72	25,2
2	26,0	5,91	4,94	0,196	0,775	8,60	21,6
3	17,4	3,94	3,28	0,131	0,531	6,51	15,4
5	10,7	2,39	1,99	0,079	0,325	4,54	9,91
6,9	7,67	1,72	1,43	0,057	0,238	3,58	7,50
10,4	5,10	1,15	0,946	0,038	0,159	2,63	5,25
14,9	3,60	0,786	0,648	0,027	0,112	1,99	3,83

what smaller (by 20%) than in the case of the Hylleraas wave functions,<sup>4</sup> while the cross section  $\sigma_{(\bar{1}0)+(\bar{1}1)}$  in our calculations is 5–10% higher.

Table II lists characteristic angles  $\theta_{\frac{1}{2}}$  for which the maximum of the function  $\sin^2 \theta(d\sigma(\theta)/d\Omega)$  is achieved. The position of this maximum coincides with the angle  $\theta_{\frac{1}{2}}(\Delta \approx 2-3\%)$  satisfying the condition  $d\sigma(\theta_{\frac{1}{2}})/d\Omega = 0.5d\sigma(0)/d\Omega$ . In the case of  $(\bar{1}\bar{1})$ -process the angle  $\theta_{\frac{1}{2}}^{(\bar{1}\bar{1})}$  corresponds to the first maximum of this function. In Table III a notation  $\sigma_{00} = \sigma_{00}(1s) + \sigma_{00}(2s) + \sigma_{00}(2p)$  is introduced, and the angle  $\theta_{\frac{1}{2}}^{(00)}$  is determined for a similar sum of differential cross sections (Table II).

We have found the following energy dependence of characteristic scattering angles:  $\theta_{\frac{1}{2}}^{(11)} \sim E^{-1}$  and  $\theta_{\frac{1}{2}}^{(00)} \sim E^{-0.5}$ . In the asymptotic region for  $E \geq 1$  MeV and processes involving negative  $H^-$  ions this dependence tends to the form  $\theta_{\frac{1}{2}}^{(\bar{1}0)+(\bar{1}1)} \sim E^{-0.5}$  and  $\theta_{\frac{1}{2}}^{(\bar{1}\bar{1})} \sim E^{-1}$ . However, the measurements carried out in Ref. 6 show that near  $E \sim 100$  KeV  $\theta_{\frac{1}{2}}^{(\bar{1}0)} \sim E^{-0.5}$ , while, according to our calculations, in this energy range  $\theta_{\frac{1}{2}}^{(\bar{1}0)} \sim E^{-1}$ , i.e. in this case the Born approximation gives a wrong result.

Note that the characteristic scattering angles  $\theta_{\frac{1}{2}}^{(00)}$  are 2 to 5 times higher than the scattering angles for hydrogen atoms formed in neutralization of  $H^-$  ions. This result needs experimental verification. However, not all scattering characteristics given by theory allow direct experimental determination. Restrictions arising here are "technical" rather than fundamental and are related to capabilities of the specific experimental setup. Thus, for example, in the present study the measurements, as mentioned above, were carried out on a ribbonlike ion beam, which can yield quantitative results concerning total cross sections of particle scattering, but gives only indirect information on characteristic angles and the form of differential cross sections for various interaction processes. In fact, the SAD of a ribbon like beam scattered by a target is a superposition of elementary distribution of  $d\sigma/d\Omega$  form. As a result, the measured SAD can differ substantially in form and parameters from the differential scattering cross section (in particular, this is the main reason why it is impossible to measure the angle  $\theta_0$  for the  $(\bar{1}\bar{1})$ -process).

To compare the theoretical differential cross section with experimental data for the SAD of the band beam (the

characteristic angle and form), it is necessary to calculate, for a given target of effective thickness  $t$ , the SAD of the band beam, using theoretical cross sections  $d\sigma/d\Omega$ , and then compare it with the measured distribution. This has been done to check indirectly the values of  $\theta_{\downarrow}^{(00)}$  from Table II for a helium target, single particle collisions, and two values of hydrogen atom energy:  $E = 1.15$  and  $1.67$  MeV. It has been found that in both cases the width and form of the SAD of a band beam of hydrogen atoms measured to experimental accuracy of  $\pm 50\%$  coincides with the width and form of the distribution calculated on the basis of the theoretical differential cross section  $d\sigma_{00}(\theta)/d\Omega$  being the result of the present study. Further discussion of angular measurements, comprising the subject of separate studies, is beyond the scope of this paper.

Note also that the angles  $\theta_{\downarrow}^{(\bar{1}0) + (\bar{1}1)}$  calculated by us are  $\sim 1.5$  times larger than those measured in Ref. 6 and smaller by about the same factor than the angles calculated in Ref. 4. This means that a simple Chandrasekar wave function can be successfully used in calculations of cross sections and characteristic scattering angles for  $H^-$  ions.

As seen from Table III, the partial cross sections for the (00)-process are arranged in the following order:  $\sigma_{00}(1s) > \sigma_{00}(2p) > \sigma_{00}(2s)$ . As to the energy dependence of total cross sections, we have  $\sigma_{(\bar{1}0) + (\bar{1}1)}$  and  $\sigma_{00} \sim E^{-1}$  (for  $E \gtrsim 1$  MeV),  $\sigma_{11} \sim (\ln E)/E$ , and  $\sigma_{\bar{1}\bar{1}} \sim E^{-0.75}$  ( $E = 3 \dots 15$  MeV).

## CONCLUSIONS

1. Comparing the cross sections  $\sigma_{ii}$  found theoretically and in experiment (Table I), we see that, within the mea-

surement error, their values satisfactorily agree with each other.

2. The cross sections and characteristic angles for the considered processes of particle interaction with and without charge changing are so related that the effect of (ii) processes on the formation of a hydrogen atom or proton beam can, in some practical cases, be of importance. It is evident that the role of (ii)-processes should be estimated for any combination of incident particles and targets.

3. From a practical point of view, it is useful to extend the study of (ii)-processes to targets of alkali metal vapors, molecules with high electric dipole moment, and to plasma targets.

In conclusion I express my gratitude to G. D. Ved'manov and B. V. Shul'gin for their interest in my study and invaluable help, and also to A. A. Babanin, V. N. Kudryavtsev, Yu. G. Lazarev, and others for help with the experiment.

<sup>1</sup>H. S. W. Massey and E. H. S. Burhop, *Electronic and Ionic Impact Phenomena*, Oxford, 1952.

<sup>2</sup>G. D. Ved'manov, V. P. Kozlov, V. N. Kudryavtsev *et al.* Prib. Tekh. Eksp. [Instrum. Exp. Tech. (USSR)] **2**, 47 (1989).

<sup>3</sup>N. V. Fedorenko, Zh. Tekh. Fiz. **40**, 2481 (1970) [Sov. Phys. Tech. Phys. **15**, 1947 (1971)].

<sup>4</sup>Y. T. Lee and J. C. Y. Chen, Phys. Rev. A **19**, 526 (1979).

<sup>5</sup>H. S. W. Massey, *Negative Ions*, 3d ed. University Press, Cambridge, 1976.

<sup>6</sup>B. A. Dyachkov, V. I. Zinenko, and G. V. Kazantsev, Zh. Tekh. Fiz. **47**, 416, 1977 [Sov. Phys. Tech. Phys. **22**, 245 (1977)].

Translated by E. Khmel'nitski